SARCOIDOSIS VASCULITIS AND DIFFUSE LUNG DISEASES 2017; 34; 315-325

Assessment of lung involvement in sarcoidosis – the use of an open-source software to quantify data from computed tomography

Tomaz Urbankowski[1], Lucyna Opoka[2], Paweł Wojtan[1], Rafal Krenke[1]

[1] Department of Internal Medicine, Pulmonary Diseases and Allergy, Medical University of Warsaw, Poland; [2] Department of Radiology, National Tuberculosis and Lung Diseases Research Institute, Warsaw, Poland

Abstract. Computed tomography (CT) plays a pivotal role in the initial evaluation of patients suspected of sarcoidosis. Although it has significant limitations associated with radiation exposure, CT scanning is also occasionally used to follow-up patients with sarcoidosis. Hitherto, no widely accepted method of quantitative assessment of pulmonary involvement in sarcoidosis has been established. The aims of the study were as follows: (1) to assess the utility of the open-source, free of charge DICOM Viewer software in quantitative analysis of pulmonary involvement in sarcoidosis; (2) to compare the parameters of quantitative CT analysis with the results of pulmonary function tests (PFTs). We included contrast-enhanced thorax CT examinations of 80 patients with sarcoidosis. Post-processing analysis of CT data was carried out using OsiriX Lite software (Pixmeo, Switzerland). Following densitometric parameters were measured: CT-derived lung volume (CT-LV), mean lung attenuation (MLA), kurtosis, skewness and standard deviation of lung radiodensity (SD_{LR}). Kurtosis was significantly lower in patients with lung fibrosis comparing to those with mediastinal and/or hilar lymphadenopathy (MHL) and pulmonary involvement (median 1.49 vs 1.93). Furthermore, SD_{LR} was significantly higher in patients with lung fibrosis comparing to those with isolated MHL and MHL with pulmonary involvement (median 163.6 vs 137.4). Also, significant correlations between densitometric parameters and the results of PFTs were demonstrated, including correlation between CT-LV and TLC (R=0.7). Our study showed that post-processing of the CT data with the use of Osirix Lite DICOM Viewer might be a valuable method of quantitative analysis of pulmonary involvement in sarcoidosis. *(Sarcoidosis Vasc Diffuse Lung Dis 2017; 34: 315-325)*

Key words: pulmonary, sarcoidosis, interstitial, lung diseases, multidetector computed tomography, image processing, computer-assisted

Introduction

Sarcoidosis is a multiorgan granulomatous disease of unknown origin most commonly affecting the lungs. Hence, chest imaging plays a crucial role in making the diagnosis in nearly all patients. Imaging methods are also useful in the follow-up of patients with sarcoidosis. The classical radiographic features of sarcoidosis have been recapitulated by J.G. Scadding and presented as a staging system (1). This system was based on plain chest radiograph. As chest radio-

Received: 23 August 2017
Accepted after revision: 5 December 2017
Correspondence: Prof. Rafał Krenke, MD, PhD
Department of Internal Medicine,
Pulmonary Diseases and Allergy,
Medical University of Warsaw
Postal address: ul. Banacha 1a, Warsaw
Postal code: 02-097
Tel. +48 22 599 2562
Fax: +48 22 599 1560
E-mail: rafalkrenke@interia.pl

graph is characterized by a relatively low sensitivity, it has currently been largely replaced by spiral and high resolution computed tomography (HRCT). The use of HRCT is particularly recommended in symptomatic patients, those with impaired pulmonary function and/or atypical radiographic findings (2-4). The most common CT findings in pulmonary sarcoidosis include: mediastinal and/or hilar lymphadenopathy (MHL), parenchymal lesions including nodules with subpleural, perilymphatic and peribronchovascular distribution, reticular and/or ground-glass opacities as well as lung fibrosis with honeycombing typically in the middle and upper lung zones (2).

Computed tomography is an invaluable method in the initial evaluation of patients suspected of sarcoidosis. It serves as a guide and a navigational tool for planning biopsy procedures, e.g. endobronchial ultrasound guided transbronchial needle aspiration (EBUS-TBNA) of the mediastinal lymph nodes or transbronchial lung biopsy. Although HRCT is associated with relatively high doses of ionizing radiation, it is occasionally used to monitor the pulmonary involvement in sarcoidosis. This refers, in particular, to patients with new radiographic findings and/or deterioration of the results of pulmonary function tests (PFTs). Hitherto, no widely accepted system of quantitative assessment of pulmonary involvement in sarcoidosis has been established (3, 5). Thus, there is a need for an easily available and objective tool that can quantify the extent/severity of pulmonary sarcoidosis. This system might be useful in both clinical practice and research studies. In recent years, different open-source DICOM (Digital Imaging and Communications in Medicine) viewers for personal computers have been developed. OsiriX is one of the most advanced, certified and validated software for clinical use in medicine (6, 7). This iOS dedicated software offers full image manipulation such as zoom, pan and window level using gesture, as well as segmentation of the anatomical structures and complex imaging analysis (8). With OsiriX, pulmonary parenchyma can be segmented and the area of increased attenuation that reflects sarcoid lung lesions or fibrosis can be calculated (8, 9).

The aims of the study were as follows: (1) to assess the utility of the open source, free of charge DICOM Viewer software (OsiriX Lite, Pixmeo, Switzerland) in the quantitative analysis of pulmonary involvement in sarcoidosis; (2) to compare the parameters of quantitative CT analysis with the results of pulmonary function tests.

Material and methods

General study design

This was a *post hoc* analysis of data collected during a prospective study on bronchoscopic sampling techniques in sarcoidosis. We performed qualitative and quantitative assessment of chest CT examinations and compared results of CT examinations with PFTs results. The study was approved by the institutional review board and registered at ClinicalTrials.gov (NCT01836822).

Patients

A flowchart presenting the process of patient and CT scan selection for analysis is presented in Figure 1. One hundred forty two consecutive patients referred to our institution between 2009 and 2015 with suspicion of sarcoidosis were subjected for initial evaluation. In 126 patients, sarcoidosis was diagnosed on the basis of compatible clinical findings and histologic demonstration of noncaseating granulomas according to international guidelines (10). Only those patients were selected for further analysis. The additional inclusion criteria were as follows: age >18 years, exclusion of other granulomatous pulmonary diseases (e.g. tuberculosis) and comorbidities that could have affected lung parenchyma (e.g. heart failure). Then, pre-bronchoscopy chest computed tomography scans were downloaded from hospital picture archiving and communication system (PACS) to a local MacBook Pro computer (processor Intel Core i5 2.3 GHz, OS X Yosemite operating system, version 10.10.3). All 126 scans were analyzed to select series meeting the following criteria: spiral, thin section (slice thickness ≤1.5 mm) investigations including contiguous slices, no radiological features of concomitant respiratory and/or heart diseases, no respiratory artifacts. Using the above criteria chest CT scans of 32 patients had to be excluded from the study. Among the remaining 94 scans, there were 80 and 14 contrast enhanced scans and non-contrast scans, respectively. Providing the impact of radiocontrast agent on computed

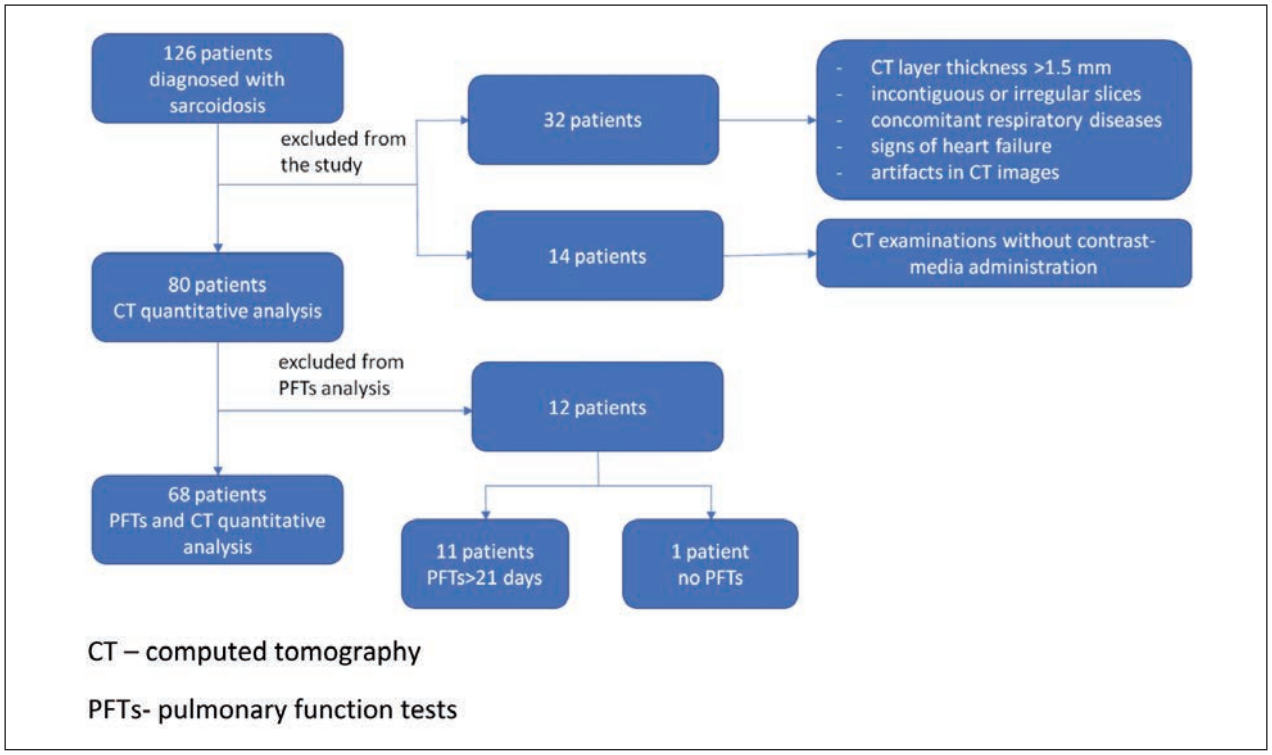

Fig. 1. Flowchart presenting the patient inclusion to the study

tomography-derived quantitative indices (CT-QI), only contrast-enhanced examinations of 80 patients with sarcoidosis were included in the final analysis.

Characteristics of CT imaging

Spiral thin-section CT (sTSCT) examinations were performed with 16 or 64-row multidetector computed tomography scanners (Light Speed 16 PRO or Optima CT 660 - General Electric, Milwaukee, WI, USA.). Following settings were used: 120 kVp, 150-300 mAs, pitch 0.938-0.984 and a reconstruction interval of 1.25 mm. Acquisition of continuous sections was started at peak inspiration after automated contrast injection and was performed in the cranio-caudal direction. The sTSCT image data were reconstructed with a high spatial frequency algorithm and analyzed at a window width (WW) of 1500 Hounsfield units (HU) and a window level (WL) of –700 HU.

sTSCT qualitative assessment

Qualitative assessment of the chest sTSCT scans was performed by a radiologist (LO) with 25 years of experience in pulmonary imaging. The commercial workstation MDRC-1119 (Barco, Belgium), was used to display and analyze the images. sTSCT scans were specifically assessed in terms of MHL, interstitial lung involvement and lung fibrosis. Based on the results of sTSCT the patients were classified into the following categories: A – isolated MHL, B – MHL with pulmonary involvement, C – lung involvement without MHL and D – lung fibrosis. In case of ambiguous sTSCT findings, the images were reviewed and discussed with the senior staff of the Department of Radiology in order to reach the consensus.

sTSCT quantitative assessment

Post-processing analysis of sTSCT data was carried out using open-source free software OsiriX Lite (version 7.5.1, Pixmeo, Switzerland) on a MacBook Pro (processor Intel Core i5 2.3 GHz, OS X Yosemite operating system, version 10.10.3). To perform lung segmentation, previously established radiodensity values of pulmonary parenchyma (be-

tween -200 and -1024 Hounsfield units, HU) were adopted and CT-derived lung volume was calculated (CT-LV) (11). The following densitometric parameters reported previously as useful in the assessment of pulmonary involvement in interstitial lung diseases (ILD) were measured: mean lung attenuation (MLA), kurtosis, skewness and standard deviation of lung radiodensity (SD_{LR}) (8, 12). All of the above parameters were calculated using method reported by Ariani et al. (8). To increase the specificity of lung parenchyma assessment a minimal manual correction of automatic segmentation was made by a single observer. This was done in order to exclude non-parenchymal structures with radiodensity within the adopted ranges, i.e. trachea, major blood vessels, main and lobar bronchi. Figure 2 shows the OsiriX Lite lung segmentation in one patient with sarcoidosis with MHL and pulmonary involvement.

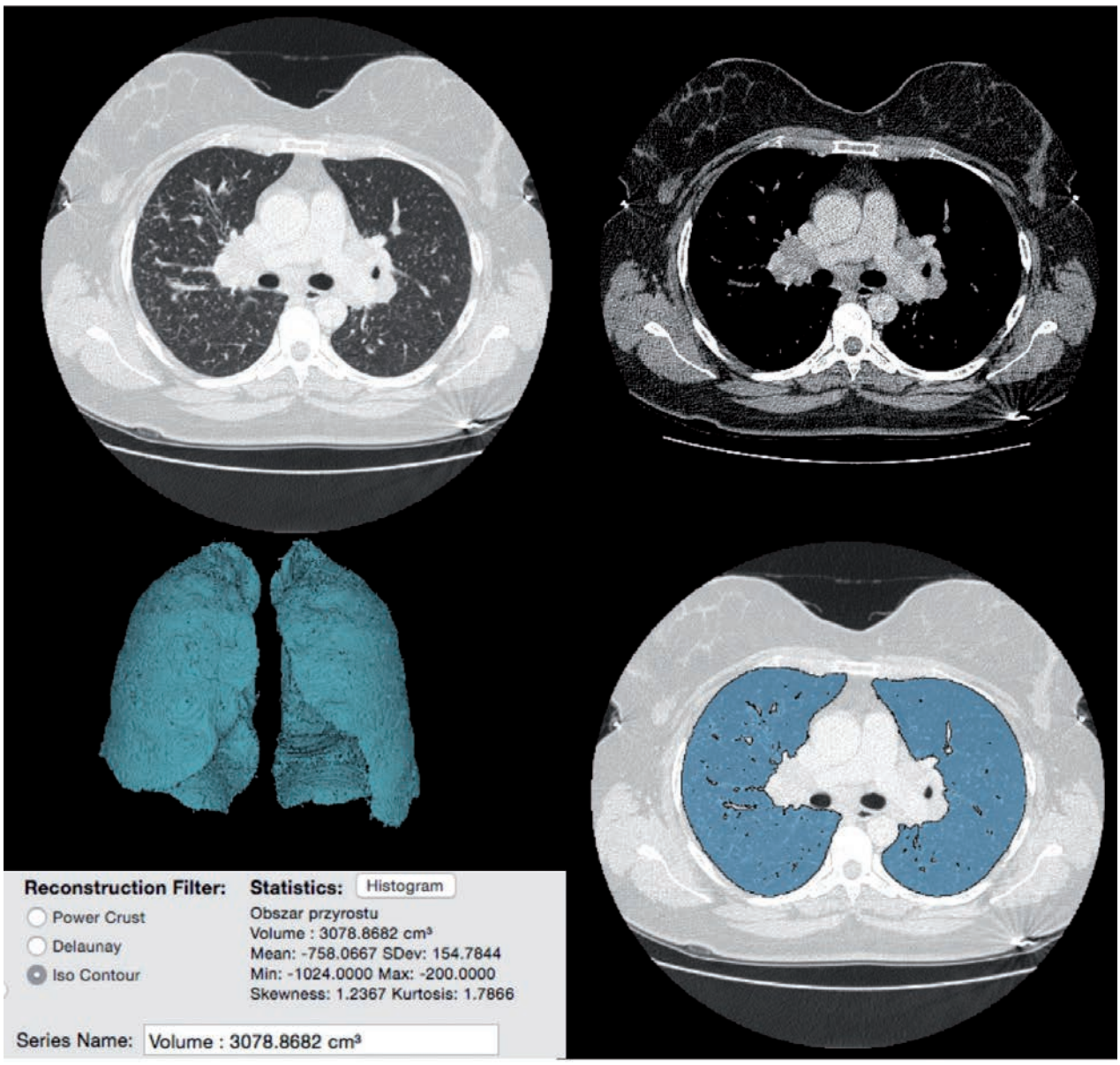

Fig. 2. Lung segmentation in a patient with mediastinal and hilar lymph node enlargement and pulmonary involvement

Pulmonary function testing

In 68 patients, the results of pulmonary function tests (PFTs) performed within 3 weeks from sTSCT examination were available. These included spirometry, body plethysmography and lung diffusion capacity for carbon monoxide. All pulmonary function measurements were performed in the local PFT laboratory (using BodyBox 5500 device, Medisoft, Sorinnes, Belgium) according to international standards (13-15). Actual values and percent of predicted of the following parameters were included in the analysis: forced vital capacity (FVCact and FVC%pred, respectively), forced expiratory volume in first second (FEV_1act, FEV_1%pred, respectively), total lung capacity (TLC act, TLC%pred, respectively), lung diffusion capacity for carbon monoxide (DL_{CO}act, DL_{CO}%pred).

Statistical analysis

Statistical analysis was performed using Statistica software package (version 12.0, StatSoft Inc., Tulsa, USA). Data are presented as medians and interquartile ranges (IQR). Differences between quantitative variables in independent groups were tested with Kruskal-Wallis test and *post-hoc* Dunn's test. Receiver Operating Characterstic (ROC) curve analysis was performed to assess the discriminative power of each CT-QI with respect to the lung involvement detected on sTSCT images by radiologist. Differences between lung volumes calculated using sTSCT images and measured by PFTs were assessed using Wilcoxon's test. Correlations between quantitative parameters were expressed as Spearman's rank correlation coefficient. A p value below 0.05 was considered statistically significant.

Results

Study group characteristics and qualitative sTSCT results

The study group comprised of 36 women and 44 men, median age 40 years (IQR 32-47.5). Distribution of patients with different radiographic stages of sarcoidosis (A-D) is presented in Figure 3. There were no patients in C category, i.e. lung interstitial involvement with no concomitant MHL. The vast majority of patients were classified into B category.

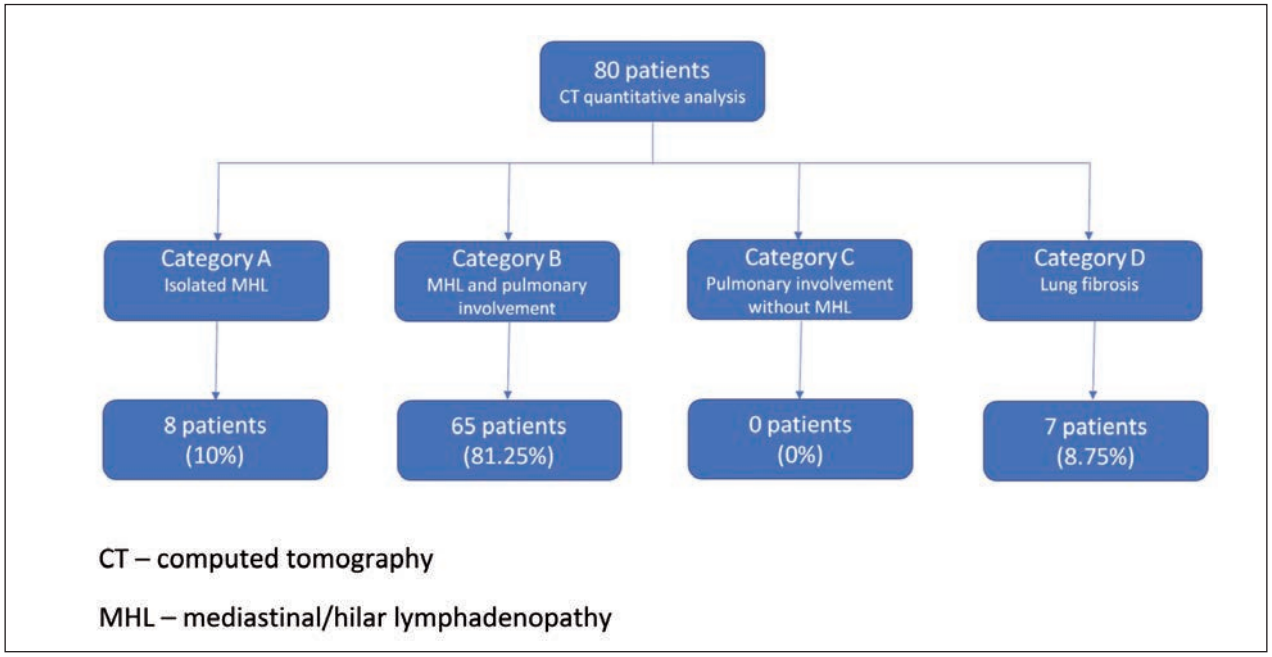

Fig. 3. Flowchart presenting the results of qualitative CT analysis

Quantitative sTSCT assessment

Comparison of different CT-derived quantitative indices (CT-QI) in patients with different radiographic patterns of sarcoidosis (A-D categories) is presented in Table 1. Kurtosis and SD_{LR} differed significantly between patients assigned to categories A, B and D. Kurtosis was significantly lower in patients with lung fibrosis (category D) comparing to those with MHL and pulmonary involvement assigned to category B (Figure 4). Furthermore, SD_{LR} was significantly higher in patients in category D (lung fibrosis) comparing to those in categories A and B (Figure 4). Skewness and MLA did not differ significantly between categories A, B and D.

Comparison of PFTs and sTSCT results

We found significant differences in FVC%pred, FEV_1%pred and DL_{CO}%pred among patients assigned to categories A, B and D (Table 2); with FVC%pred and FEV_1%pred being significantly lower in patients with lung fibrosis than in patients classified as A and B categories. Moreover, DL_{CO}%pred was significantly lower in patients in categories B and D comparing to those with isolated MHL. Also, significant correlations between CT-LV, SD_{LR}, skewness and kurtosis and the results of PFTs were demonstrated (Table 3). Interestingly, TLCact and FVCact correlated with all above CT-QI. On the other hand, the only parameter that significantly correlated with DL_{CO}act and DL_{CO}%pred was CT-LV. A strong positive correlation (R=0.77, p<0.0001) between CT-LV and TLCact was found (Figure 5). However, CT-LV and TLCact differed significantly (p<0.0001). The median CT-LV

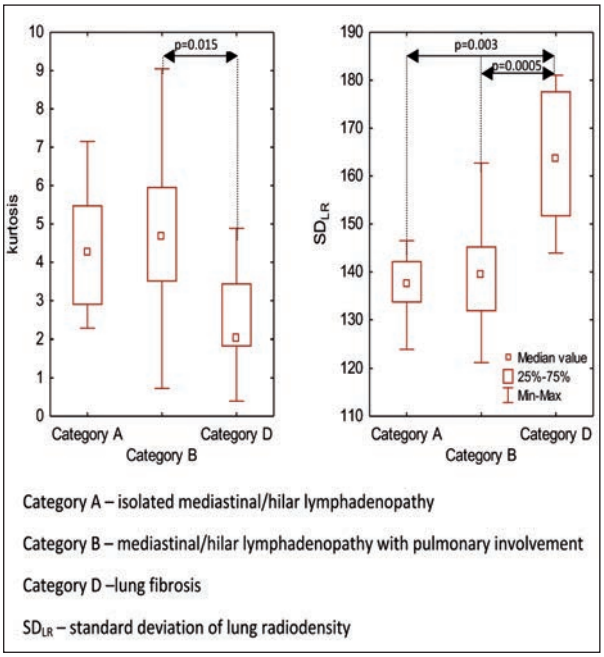

Fig. 4. Kurtosis and standard deviation of lung radiodensity in patients classified into A, B and D categories

Table 1. CT-derived quantitative indices in patients with different imaging findings

	Category A *Isolated MHL* (n=8, 10%)	Category B *MHL with pulmonary involvement* (n=65, 81.25%)	Category D *Lung fibrosis* (n=7, 8.75%)	
CT-LV (L)	4.8 (IQR 4.02-6.21)	5.14 (IQR 4.45-6.01)	5.11 (IQR 3.56-5.81)	NS
SD_{LR}	137.4 (IQR 133.6-142.3)	139.5 (IQR 131.8-145.3)	163.6 (IQR 151.6-177.7)	p=0.0006 p^{A-B}>0.05 p^{A-D}=0.003 p^{B-D}=0.0005
Skewness	1.93 (IQR 1.71-2.28)	1.94 (IQR 1.71-2.15)	1.49 (IQR 1.42-1.97)	NS
Kurtosis	4.25 (IQR 2.9-5.49)	4.68 (IQR 3.50-5.97)	2.02 (IQR 1.82-3.45)	p=0.003 p^{A-B}>0.05 p^{A-D}>0.05 P^{B-D}=0.015
MLA (HU)	-769.8 (IQR -820.9-[-740.1])	-815 (IQR -832.6-[-794.3])	-803.2 (IQR -812-[-787.3])	NS

MHL – mediastinal/hilar lymph node enlargement; CT-LV – computed tomography-derived lung volume; SD_{LR} – standard deviation of lung radiodensity; MLA – mean lung attenuation; HU – Hounsfield units; PFF – pulmonary fibrosis fraction; NS – no significant difference in Kruskal-Wallis test; p – value in Kruskal-Wallis test, p^{A-B}, p^{A-D}, p^{B-D} – values in Dunn's tests (comparison between A-B, A-D and B-D, respectively)

Table 2. Results of pulmonary function tests performed within 3 weeks from tomography in 68 patients with different imaging findings

	Category A *Isolated MHL* (n=6, 8.82%)	Category B *MHL with pulmonary involvement* (n=57, 83.82%)	Category D *Lung fibrosis* (n=5, 7.35%)	
FVC%pred	117 (98.7-138.1)	108.1 (99.5-122.6)	85 (84.5-95)	p=0.028 p^{A-B}>0.05 p^{A-D}=0.049 p^{B-D}=0.034
FEV_1%pred	110.4 (92.4-125.5)	99.8 (91.2-107.1)	71.4 (66-84.7)	p=0.01 p^{A-B}>0.05 p^{A-D}=0.009 p^{B-D}=0.028
TLC%pred	119.2 (101.7-122.6)	106.15 (97.5-116.4)	97.2 (85-110.9)	NS
DL_{CO}%pred	99.3 (93.05-111.5)	96 (84.9-106.8)	88.7 (80.8-95.2)	p=0.017 p^{A-B}=0.035 p^{A-D}=0.027 p^{B-D}>0.05

p – value in Kruskal-Wallis test, p^{A-B}, p^{A-D}, p^{B-D} – values in Dunn's tests (comparison between A-B, A-D and B-D, respectively); NS – no significant difference in Kruskal-Wallis test; MHL – mediastinal/hilar lymphadenopathy, FVC%pred- forced vital capacity, percent of predicted value; FEV_1%pred – forced expiratory volume in first second, percent of predicted value; TLC%pred – total lung capacity, percent of predicted value; DL_{CO}%pred –diffusing lung capacity for carbon monoxide, percent of predicted value

Table 3. Correlations between computed tomography-derived quantitative indices and results of pulmonary function tests

	FVC act.	FVC %pred	FEV_1 act.	FEV_1 %pred	TLC act.	TLC %pred	Dlcoact.	Dlco %pred
CT-LV	**0.7***	0.24	**0.61***	0.16	**0.77***	0.23	**0.52***	**0.31***
SD_{LR}	**-0.31***	-0.21	**-0.29***	-0.19	**-0.32***	**-0.28***	-0.1	-0.06
Skewness	**0.32***	0.14	**0.26**	0.06	**0.41***	0.19	0.10	0.03
Kurtosis	**0.32***	0.23	**0.27***	0.17	**0.4***	**0.28***	0.08	0.04

* - statistically significant in Spearman correlation test (value of Spearman's rank correlation coefficient is shown in each box)
CT-LV – computed tomography-derived lung volume; SD_{LR} – standard deviation of lung radiodensity; FVC – forced vital capacity; FEV_1 – forced expiratory volume in first second; TLC – total lung capacity; DL_{co}- diffusing capacity for carbon monoxide; act. – actual value; %pred - % of predicted value

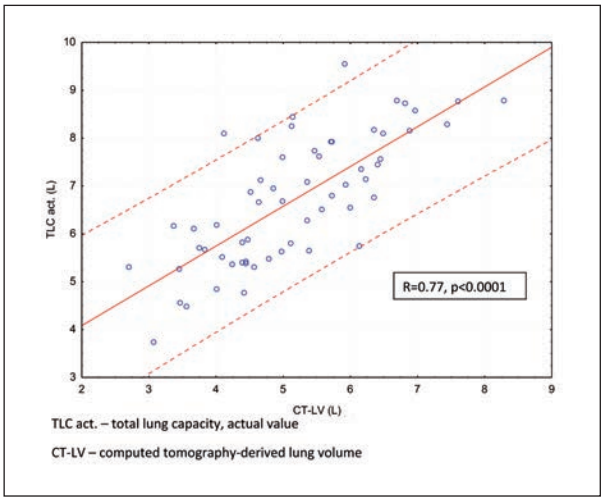

Fig. 5. Correlation between computed-tomography-derived lung volume and total lung capacity

and TLCact in 68 patients with available results of PFTs were 5.06 L (IQR 4.41-5.97) and 6.71 L (IQR 5.63-7.91), respectively.

ROC analysis performed to search for the best radiographic qualitative predictor of lung fibrosis seen in sTSCT showed the highest AUC for SD_{LR} (AUC=0.939, p=0.0000, Youden index=0.77). The best threshold value of SD_{LR} was 151.58 with the sensitivity and specificity of 85.7% and 91.8%, respectively, comparing to visual assessment of sTSTC by the radiologist.

Discussion

Our study showed that post-processing of the CT data with the use of an open-source Osirix Lite

DICOM Viewer is a valuable method of quantitative analysis of pulmonary involvement in sarcoidosis. What seems particularly important is that the quantitative analysis can be easily and reliably done not only by a radiologist but by a pulmonologist, as well. We found that CT-QI differed significantly in patients with distinct radiographic patterns of sarcoidosis and correlated with results of pulmonary function tests. We demonstrated that increased value of SD_{LR} could efficiently diagnose patients with lung fibrosis defined by the qualitative CT assessment by an experienced radiologist. Both SD_{LR} and kurtosis were shown to be more reliable densitometric parameters in the assessment of pulmonary involvement in sarcoidosis comparing to skewness and MLA. Also, lower SD_{LR} values and higher values of CT-LV, skewness and kurtosis were associated with more favorable results of PFTs.

As reliable and reproductive interpretation of CT findings in patients with ILD remains problematic not only for pulmonologists but also for radiologists, new tools that enable quantitative assessment of lung involvement may be particularly helpful in clinical practice. Thus, we believe that results of our study that used easily available free software may have real practical applications. Hitherto, the major problem with qualitative CT assessment is the lack of commonly accepted scoring systems and relatively high interobserver variability (8, 16). Having that in mind and considering radiation exposure associated with CT scanning, pulmonary function tests are used rather than CT to assess the severity of pulmonary sarcoidosis and to follow up the course of the disease (3, 17, 18). A new and interesting staging system for patients with pulmonary sarcoidosis was proposed by Walsh et al. This system integrates weighted index of PFTs variables, visual assessment of HRCT and the ratio of the main pulmonary artery diameter to ascending aorta diameter (19). This system dichotomously distinguishes patients with good and poor prognosis and may facilitate disease management decisions (19). Nonetheless, we believe that quantitative continuous CT scores may also be of some value, by allowing objective quantification of pulmonary involvement. Importantly, CT-QI were previously shown not to be significantly affected by low-dose CT protocols (20). Considering the significant correlation between CT-QI and the results of PFTs, we postulate that CT-QI may serve as the easily applicable end-point in the evaluation of disease progression both in clinical and research setting. However, this needs evaluation in further prospective studies.

To date, quantitative CT analysis has been used to evaluate lung structure in normal adults and to assess pulmonary diseases, including emphysema, asthma, chronic obstructive pulmonary disease (COPD), ILD, lung nodules and radiation-related lung injury (21-42). CT-QI were shown to correlate well with different clinical parameters of patients with ILD. These include the results of PFTs, visual CT semiquantitative assessment, cellular composition of the bronchoalveolar lavage fluid, quality of life scores and exercise tolerance. The above relationships were observed in various ILDs, i.e. idiopathic pulmonary fibrosis, pulmonary alveolar proteinosis, pulmonary involvement related to rheumatoid arthritis and systemic sclerosis (5, 9, 37, 43-53). In one previous study a very good intraobserver and interobserved agreement between CT-QI calculations was shown, despite the need for minimal manual interaction (48).

Significant correlations between parameters of computer-aided CT analysis and the results of pulmonary function tests were previously also demonstrated in sarcoidosis patients (3, 12). Erdal et al. found that lung texture score derived from two-point correlation analyses of the chest CT performed using a proprietary plug-in software, correlated significantly with FVC%pred, TLCact and DL_{CO}act (12). Handa et al. who used dedicated in-house software reported a significant negative correlation of SD_{LR} and positive correlation of kurtosis and skewness with TLCact, FVC%pred and DL_{CO}%pred (12). We found similar correlations using open-source, widely available DICOM software. In our study CT-QI correlated significantly with actual values of FVC, FEV_1 and TLC but not with FVC%pred nor FEV_1%pred. However, we observed a tendency towards correlation between CT-QI and predicted values of FVC and FEV_1 in the same direction as with actual values. The lack of statistical significance may result from relatively small number of included patients.

Ariani et al., who used the same open-source DICOM viewer demonstrated a significant negative correlation of skewness and kurtosis with the semiquantitative CT assessment of lung involvement in systemic sclerosis (9). These authors also observed lower values of kurtosis and skewness in patients with extensive lung fibrosis compared to limited dis-

ease (9). Recently, lower kurtosis and skewness were also shown to be associated with shorter transplant-free survival and increased mortality in patients with idiopathic pulmonary fibrosis (IPF) (43). Both parameters correlated positively with FVC%pred and DL_{CO}%pred (43). By contrast, when smokers with no ILD were studied, higher expiratory kurtosis and skewness correlated significantly with deteriorated lung function and more severe airflow limitation (54). It must be admitted, however, that significant variability in lung radiodensity parameters in normal subjects was also reported (11).

Surprisingly, we were not able to demonstrate any significant differences in SD_{LR} and kurtosis between patients with isolated MHL (category A) and those with MHL and interstitial lung lesions (category B). Furthermore, skewness did not differ significantly among patients classified to categories A, B and D. These findings could have been related to several factors, including low statistical power associated with unequal patient distribution and small numbers of patients classified to A and D categories. The distribution of patients was closely related to criteria we used to classify patients to four different categories. Due to the lack of a widely accepted CT-based qualitative scale of mediastinum and lung involvement in sarcoidosis, we adopted the classical Scadding radiographic criteria to sTSCT qualitative assessment. However, the use of these criteria to classify patients based on sTSCT encounters significant problems. Obviously, the sensitivity and specificity of CT is much higher than those of classic radiography in diagnosing MHL, pulmonary interstitial involvement and lung fibrosis. This particularly refers to discrete interstitial pulmonary lesions. Hence, all patients with mediastinal/hilar lymph node enlargement and even very few and very small pulmonary nodules were classified to category B, not A. This was probably the most important cause of the significant predominance of patients classified as category B. This might be confirmed by the result of an earlier study in which chest radiograph and classic radiographic criteria were used to classify patients with sarcoidosis. In that study, 50% and 45.8% of patients were classified as stage I and stage II sarcoidosis (compared to 10% and 81.25% in the current study) (55). The other factor that might have influenced the category B predominance was the fact that only patients with histopathological confirmation of sarcoid-like granulomatous changes were included in our study. In consequence, patients presenting with isolated MHL and typical Löfgren's syndrome who are less commonly referred for invasive diagnostic procedures, were probably underrepresented in the analysis. Furthermore, the use of sTSCT allowed the detection of less pronounced lung fibrosis, which would not be detected on classic chest radiographs. It may probably explain a relatively mild lung function impairment even in patients assigned to category D.

Although we selected a well-defined cohort of patients with biopsy-proven sarcoidosis, we are aware of several significant limitations of our study. Firstly, it was a single-center retrospective analysis that included a relatively small number of patients with the results of recent PFTs not available in all cases. Secondly, the pulmonary function impairment was mild or absent in vast majority of patients and no data on patients smoking status were analyzed. Thirdly, an uneven patient distribution and the use of not validated qualitative system to classify mediastinal and lung involvement (both issues discussed above) might be regarded as additional weaknesses of the study. Fourthly, the underestimation of total lung capacity calculated using computed tomography (CT-LV, computed tomography-derived lung volume) compared to that measured by body plethysmography suggests that some lung regions were probably not included during segmentation. Fifthly, in the majority of patients, there was a need for a minimal manual correction of automatic segmentation with the exclusion of non-parenchymatous lung structures. Finally, only verbal command, not spirometry-based lung volume controller was used to obtain deep inspiration and to perform CT scan during maximal lung inflation. This might also resulted in the differences between CT- LV and lung volumes measured by body pletyshmography.

Conclusions

To conclude, our study showed that the open source software (OsiriX Lite, Pixmeo, Switzerland) can be useful in the quantitative analysis of lung involvement in patients with sarcoidosis. Importantly, the procedures that should be done to calculate CT-QI (i.e. lung segmentation, manual correction, etc.)

do not require special skills of a radiologist, but can be carried out by an adequately trained pulmonologist, as well. Significant correlations between CT-QI and the results of PFTs suggest that sTSCT-based quantitative analysis might be an additional tool to assess and follow-up lung involvement in patients with sarcoidosis. Nevertheless, the results of our study should be further developed and confirmed in larger, well designed, prospective studies that include patients with the whole spectrum of sarcoidosis.

References

1. Scadding JG. Prognosis of intrathoracic sarcoidosis in England. A review of 136 cases after five years' observation. Br Med J 1961; 2(5261): 1165-72. PubMed PMID: 14497750; PubMed Central PMCID: PMCPMC1970202.
2. Carmona EM, Kalra S, Ryu JH. Pulmonary Sarcoidosis: Diagnosis and Treatment. Mayo Clin Proc 2016; 91(7): 946-54. doi: 10.1016/j.mayocp.2016.03.004. PubMed PMID: 27378039.
3. Erdal BS, Crouser ED, Yildiz V, et al. Quantitative computerized two-point correlation analysis of lung CT scans correlates with pulmonary function in pulmonary sarcoidosis. Chest 2012; 142(6): 1589-97. doi: 10.1378/chest.11-2027. PubMed PMID: 22628487; PubMed Central PMCID: PMCPMC4511386.
4. Keir G, Wells AU. Assessing pulmonary disease and response to therapy: which test? Semin Respir Crit Care Med 2010; 31(4): 409-18. doi: 10.1055/s-0030-1262209. PubMed PMID: 20665391.
5. Best AC, Lynch AM, Bozic CM, Miller D, Grunwald GK, Lynch DA. Quantitative CT indexes in idiopathic pulmonary fibrosis: relationship with physiologic impairment. Radiology 2003; 228(2): 407-14. doi: 10.1148/radiol.2282020274. PubMed PMID: 12802000.
6. Pixmeo SARL. OsiriX software website - overview section [cited 2017 May 10]. Available from: http://www.osirix-viewer.com/osirix/overview/.
7. Rosset A, Spadola L, Pysher L, Ratib O. Informatics in radiology (infoRAD): navigating the fifth dimension: innovative interface for multidimensional multimodality image navigation. Radiographics 2006; 26(1): 299-308. doi: 10.1148/rg.261055066. PubMed PMID: 16418259.
8. Ariani A, Carotti M, Gutierrez M, et al. Utility of an open-source DICOM viewer software (OsiriX) to assess pulmonary fibrosis in systemic sclerosis: preliminary results. Rheumatol Int 2014; 34(4): 511-6. doi: 10.1007/s00296-013-2845-6. PubMed PMID: 23949623.
9. Ariani A, Lumetti F, Silva M, et al. Systemic sclerosis interstitial lung disease evaluation: comparison between semiquantitative and quantitative computed tomography assessments. J Biol Regul Homeost Agents 2014; 28(3): 507-13. PubMed PMID: 25316138.
10. Hunninghake GW, Costabel U, Ando M, et al. ATS/ERS/WASOG statement on sarcoidosis. American Thoracic Society/European Respiratory Society/World Association of Sarcoidosis and other Granulomatous Disorders. Sarcoidosis Vasc Diffuse Lung Dis 1999; 16(2): 149-73. PubMed PMID: 10560120.
11. Salaffi F, Carotti M, Bosello S, et al. Computer-aided quantification of interstitial lung disease from high resolution computed tomography images in systemic sclerosis: correlation with visual reader-based score and physiologic tests. Biomed Res Int 2015; 2015: 834262. doi: 10.1155/2015/834262. PubMed PMID: 25629053; PubMed Central PMCID: PMCPMC4299560.
12. Handa T, Nagai S, Hirai T, et al. Computed tomography analysis of airway dimensions and lung density in patients with sarcoidosis. Respiration 2009; 77(3): 273-81. doi: 10.1159/000151544. PubMed PMID: 18714146.
13. Miller MR, Hankinson J, Brusasco V, et al. Standardisation of spirometry. Eur Respir J 2005; 26(2): 319-38. doi: 10.1183/09031936.05.00034805. PubMed PMID: 16055882.
14. Wanger J, Clausen JL, Coates A, et al. Standardisation of the measurement of lung volumes. Eur Respir J 2005; 26(3): 511-22. doi: 10.1183/09031936.05.00035005. PubMed PMID: 16135736.
15. Macintyre N, Crapo RO, Viegi G, et al. Standardisation of the single-breath determination of carbon monoxide uptake in the lung. Eur Respir J 2005; 26(4): 720-35. doi: 10.1183/09031936.05.00034905. PubMed PMID: 16204605.
16. Khanna D, Tseng CH, Farmani N, et al. Clinical course of lung physiology in patients with scleroderma and interstitial lung disease: analysis of the Scleroderma Lung Study Placebo Group. Arthritis Rheum 2011; 63(10): 3078-85. doi: 10.1002/art.30467. PubMed PMID: 21618205; PubMed Central PMCID: PMCPMC3183128.
17. Baughman RP, Drent M, Kavuru M, et al. Infliximab therapy in patients with chronic sarcoidosis and pulmonary involvement. Am J Respir Crit Care Med 2006; 174(7): 795-802. doi: 10.1164/rccm.200603-402OC. PubMed PMID: 16840744.
18. Wasfi YS, Rose CS, Murphy JR, et al. A new tool to assess sarcoidosis severity. Chest 2006; 129(5): 1234-45. doi: 10.1378/chest.129.5.1234. PubMed PMID: 16685014.
19. Walsh SL, Wells AU, Sverzellati N, et al. An integrated clinicoradiological staging system for pulmonary sarcoidosis: a case-cohort study. Lancet Respir Med 2014; 2(2): 123-30. doi: 10.1016/S2213-2600(13)70276-5. PubMed PMID: 24503267.
20. Sverzellati N, Zompatori M, De Luca G, et al. Evaluation of quantitative CT indexes in idiopathic interstitial pneumonitis using a low-dose technique. Eur J Radiol 2005; 56(3): 370-5. doi: 10.1016/j.ejrad.2005.05.012. PubMed PMID: 15978764.
21. Newell JD, Jr., Sieren J, Hoffman EA. Development of quantitative computed tomography lung protocols. J Thorac Imaging 2013; 28(5): 266-71. doi: 10.1097/RTI.0b013e31829f6796. PubMed PMID: 23934142; PubMed Central PMCID: PMCPMC3876949.
22. Zach JA, Newell JD, Jr., Schroeder J, et al. Quantitative computed tomography of the lungs and airways in healthy nonsmoking adults. Invest Radiol 2012; 47(10): 596-602. doi: 10.1097/RLI.0b013e318262292e. PubMed PMID: 22836310; PubMed Central PMCID: PMCPMC3703944.
23. da Silva EC, Silva AC, de Paiva AC, Nunes RA, Gattass M. Diagnosis of solitary lung nodules using the local form of Ripley's K function applied to three-dimensional CT data. Comput Methods Programs Biomed 2008; 90(3): 230-9. doi: 10.1016/j.cmpb.2008.02.003. PubMed PMID: 18403042.
24. Grydeland TB, Thorsen E, Dirksen A, et al. Quantitative CT measures of emphysema and airway wall thickness are related to D(L)CO. Respir Med 2011; 105(3): 343-51. doi: 10.1016/j.rmed.2010.10.018. PubMed PMID: 21074394.
25. Rutten EP, Grydeland TB, Pillai SG, et al. Quantitative CT: Associations between Emphysema, Airway Wall Thickness and Body Composition in COPD. Pulm Med 2011; 2011: 419328. doi: 10.1155/2011/419328. PubMed PMID: 21647214; PubMed Central PMCID: PMCPMC3100107.
26. Xie X, de Jong PA, Oudkerk M, et al. Morphological measurements in computed tomography correlate with airflow obstruction in chronic obstructive pulmonary disease: systematic review and meta-analysis. Eur Radiol 2012; 22(10): 2085-93. doi: 10.1007/s00330-012-2480-8. PubMed PMID: 22699870; PubMed Central PMCID: PMCPMC3431473.
27. Besir FH, Mahmutyazicioglu K, Aydin L, Altin R, Asil K, Gundogdu S. The benefit of expiratory-phase quantitative CT densitometry in the early diagnosis of chronic obstructive pulmonary disease.

Diagn Interv Radiol 2012; 18(3): 248-54. doi: 10.4261/1305-3825.DIR.4365-11.3. PubMed PMID: 22261851.
28. Stolk J, Putter H, Bakker EM, et al. Progression parameters for emphysema: a clinical investigation. Respir Med 2007; 101(9): 1924-30. doi: 10.1016/j.rmed.2007.04.016. PubMed PMID: 17644366.
29. Bakker ME, Stolk J, Putter H, et al. Variability in densitometric assessment of pulmonary emphysema with computed tomography. Invest Radiol 2005; 40(12): 777-83. PubMed PMID: 16304481.
30. Busacker A, Newell JD, Jr., Keefe T, et al. A multivariate analysis of risk factors for the air-trapping asthmatic phenotype as measured by quantitative CT analysis. Chest 2009; 135(1): 48-56. doi: 10.1378/chest.08-0049. PubMed PMID: 18689585; PubMed Central PMCID: PMCPMC2849984.
31. Jain N, Covar RA, Gleason MC, Newell JD, Jr., Gelfand EW, Spahn JD. Quantitative computed tomography detects peripheral airway disease in asthmatic children. Pediatr Pulmonol 2005; 40(3): 211-8. doi: 10.1002/ppul.20215. PubMed PMID: 16015663.
32. Newman KB, Lynch DA, Newman LS, Ellegood D, Newell JD, Jr. Quantitative computed tomography detects air trapping due to asthma. Chest 1994; 106(1): 105-9. PubMed PMID: 8020254.
33. Xu Y, van Beek EJ, Hwanjo Y, Guo J, McLennan G, Hoffman EA. Computer-aided classification of interstitial lung diseases via MDCT: 3D adaptive multiple feature method (3D AMFM). Acad Radiol 2006; 13(8): 969-78. doi: 10.1016/j.acra.2006.04.017. PubMed PMID: 16843849.
34. Hoffman EA, Reinhardt JM, Sonka M, et al. Characterization of the interstitial lung diseases via density-based and texture-based analysis of computed tomography images of lung structure and function. Acad Radiol 2003; 10(10): 1104-18. PubMed PMID: 14587629.
35. Uppaluri R, Hoffman EA, Sonka M, Hunninghake GW, McLennan G. Interstitial lung disease: A quantitative study using the adaptive multiple feature method. Am J Respir Crit Care Med 1999; 159(2): 519-25. doi: 10.1164/ajrccm.159.2.9707145. PubMed PMID: 9927367.
36. Beinert T, Kohz P, Seemann M, Egge T, Reiser M, Behr J. Spirometrically controlled high resolution computed tomography - quantitative assessment of density distribution in patients with diffuse fibrosing alveolitis. Eur J Med Res 1996; 1(6): 269-72. PubMed PMID: 9367938.
37. Hartley PG, Galvin JR, Hunninghake GW, et al. High-resolution CT-derived measures of lung density are valid indexes of interstitial lung disease. J Appl Physiol (1985) 1994; 76(1): 271-7. PubMed PMID: 8175517.
38. Sieren JC, Smith AR, Thiesse J, et al. Exploration of the volumetric composition of human lung cancer nodules in correlated histopathology and computed tomography. Lung Cancer 2011; 74(1): 61-8. doi: 10.1016/j.lungcan.2011.01.023. PubMed PMID: 21371772; PubMed Central PMCID: PMCPMC3129434.
39. Petkovska I, Shah SK, McNitt-Gray MF, et al. Pulmonary nodule characterization: a comparison of conventional with quantitative and visual semi-quantitative analyses using contrast enhancement maps. Eur J Radiol 2006; 59(2): 244-52. doi: 10.1016/j.ejrad.2006.03.005. PubMed PMID: 16616822; PubMed Central PMCID: PMCPMC1618788.
40. Palma DA, van Sornsen de Koste J, Verbakel WF, Vincent A, Senan S. Lung density changes after stereotactic radiotherapy: a quantitative analysis in 50 patients. Int J Radiat Oncol Biol Phys 2011; 81(4): 974-8. doi: 10.1016/j.ijrobp.2010.07.025. PubMed PMID: 20932655.
41. Mah K, Van Dyk J. Quantitative measurement of changes in human lung density following irradiation. Radiother Oncol 1988; 11(2): 169-79. PubMed PMID: 3353521.
42. Sumikawa H, Johkoh T, Yamamoto S, et al. Computed tomography values calculation and volume histogram analysis for various computed tomographic patterns of diffuse lung diseases. J Comput Assist Tomogr 2009; 33(5): 731-8. doi: 10.1097/RCT.0b013e31818da65c. PubMed PMID: 19820502.
43. Ash SY, Harmouche R, Vallejo DL, et al. Densitometric and local histogram based analysis of computed tomography images in patients with idiopathic pulmonary fibrosis. Respir Res 2017; 18(1): 45. doi: 10.1186/s12931-017-0527-8. PubMed PMID: 28264721; PubMed Central PMCID: PMCPMC5340000.
44. Rienmuller RK, Behr J, Kalender WA, et al. Standardized quantitative high resolution CT in lung diseases. J Comput Assist Tomogr 1991; 15(5): 742-9. PubMed PMID: 1885791.
45. Marten K, Dicken V, Kneitz C, et al. Computer-assisted quantification of interstitial lung disease associated with rheumatoid arthritis: preliminary technical validation. Eur J Radiol 2009; 72(2): 278-83. doi: 10.1016/j.ejrad.2008.07.008. PubMed PMID: 18722728.
46. Sverzellati N, Calabro E, Chetta A, et al. Visual score and quantitative CT indices in pulmonary fibrosis: Relationship with physiologic impairment. Radiol Med 2007; 112(8): 1160-72. doi: 10.1007/s11547-007-0213-x. PubMed PMID: 18193399.
47. Best AC, Meng J, Lynch AM, et al. Idiopathic pulmonary fibrosis: physiologic tests, quantitative CT indexes, and CT visual scores as predictors of mortality. Radiology 2008; 246(3): 935-40. doi: 10.1148/radiol.2463062200. PubMed PMID: 18235106.
48. Camiciottoli G, Orlandi I, Bartolucci M, et al. Lung CT densitometry in systemic sclerosis: correlation with lung function, exercise testing, and quality of life. Chest 2007; 131(3): 672-81. doi: 10.1378/chest.06-1401. PubMed PMID: 17356079.
49. Shin KE, Chung MJ, Jung MP, Choe BK, Lee KS. Quantitative computed tomographic indexes in diffuse interstitial lung disease: correlation with physiologic tests and computed tomography visual scores. J Comput Assist Tomogr 2011; 35(2): 266-71. doi: 10.1097/RCT.0b013e31820ccf18. PubMed PMID: 21412102.
50. Salaffi F, Carotti M, Di Donato E, Di Carlo M, Ceccarelli L, Giuseppetti G. Computer-Aided Tomographic Analysis of Interstitial Lung Disease (ILD) in Patients with Systemic Sclerosis (SSc). Correlation with Pulmonary Physiologic Tests and Patient-Centred Measures of Perceived Dyspnea and Functional Disability. PLoS One 2016; 11(3): e0149240. doi: 10.1371/journal.pone.0149240. PubMed PMID: 26930658; PubMed Central PMCID: PMCPMC4773230.
51. Perez At, Coxson HO, Hogg JC, Gibson K, Thompson PF, Rogers RM. Use of CT morphometry to detect changes in lung weight and gas volume. Chest 2005; 128(4): 2471-7. doi: 10.1378/chest.128.4.2471. PubMed PMID: 16236911.
52. Salaffi F, Fraticelli P, Carotti M, et al. Internal and external responsiveness of computer-aided quantification of interstitial lung disease from high resolution computed tomography images in systemic sclerosis: a comparison with visual Reader-Based score Sarcoidosis Vasculitis and Diffuse Lung Diseses 2017; 34(1): 18-25.
53. Camiciottoli G, Diciotti S, Bartolucci M, et al. Whole-lung volume and density in spirometrically-gated inspiratory and expiratory CT in systemic sclerosis: correlation with static volumes at pulmonary function tests. Sarcoidosis Vasc Diffuse Lung Dis 2013; 30(1): 17-27. PubMed PMID: 24003531.
54. Yamashiro T, Matsuoka S, Estepar RS, et al. Kurtosis and skewness of density histograms on inspiratory and expiratory CT scans in smokers. COPD 2011; 8(1): 13-20. doi: 10.3109/15412555.2010.541537. PubMed PMID: 21299474.
55. Domagala-Kulawik J, Urbankowski T, Safianowska A. S Fas in bronchoalveolar lavage fluid of patients with sarcoidosis in relation to cigarette smoking. Hum Immunol 2013; 74(7): 858-60. doi: 10.1016/j.humimm.2013.04.015. PubMed PMID: 23619472.